

# Patterns of intraplate volcanism controlled by asthenospheric shear

Clinton P. Conrad<sup>1\*</sup>†, Todd A. Bianco<sup>1†</sup>, Eugene I. Smith<sup>2</sup> and Paul Wessel<sup>1</sup>

**Most of Earth's volcanism occurs at plate boundaries, in association with subduction or rifting. A few high-volume volcanic fields are observed both at plate boundaries and within plates, fed by plumes upwelling from the deep mantle<sup>1</sup>. The remaining volcanism is observed away from plate boundaries. It is typically basaltic, effusive and low volume, occurring within continental interiors<sup>2–7</sup> or creating seamounts on the ocean floor<sup>8–11</sup>. This intraplate volcanism has been attributed to various localized processes<sup>12</sup> such as cracking of the lithosphere<sup>8,13,14</sup>, small-scale convection in the mantle beneath the lithosphere<sup>15–17</sup> or shear-induced melting of low-viscosity pockets of asthenospheric mantle that have become embedded along the base of the lithosphere<sup>18</sup>. Here we compare the locations of observed intraplate volcanism with global patterns of mantle flow from a numerical model. We find a correlation between recent continental and oceanic intraplate volcanism and areas of the asthenosphere that are experiencing rapid shear due to mantle convection. We detect particularly high correlations in the interior of the continents of western North America, eastern Australia, southern Europe and Antarctica, as well as west of the East Pacific Rise in the Pacific Ocean. We conclude that intraplate volcanism associated with mantle convection is best explained by melting caused by shear flow within the asthenosphere, whereas other localized processes are less important.**

Low-volume effusive volcanism occurring within plate interiors<sup>2</sup> cannot be attributed to either plate boundary processes or upwelling mantle plumes<sup>1</sup>, and thus defies a ready explanation<sup>12</sup>. Regionalized and diffuse extension leading to asthenospheric upwelling and melting<sup>3</sup> has been invoked as a tectonic explanation, but recent studies have suggested that lithospheric extension may actually impede mantle melting<sup>14</sup>. Intraplate volcanism has also been attributed to several locally operating subsurface processes, such as minor upwelling plumes<sup>15</sup>, downwelling drips<sup>16</sup> and sub-lithospheric<sup>17</sup> or edge-driven<sup>15</sup> convection, that invoke local density heterogeneity to draw hot mantle upwards where it can decompress and melt. Discussions about the relative importance of these mechanisms arise partly because local control of intraplate volcanism disconnects it from the globally unifying processes of mantle convection and plate tectonics.

However, several mechanisms may connect global mantle flow and plate motions to sub-lithospheric melting within plate interiors. For example, a rapidly shearing asthenosphere may amplify tractions on the base of the tectonic plates<sup>19</sup>, inducing cracking and other volcanism-inducing deformations<sup>2,8,13</sup>. Alternatively, rapid asthenospheric deformation may weaken the lower lithosphere if its rheology is non-Newtonian, inducing

convective instabilities<sup>20</sup> that can induce surface volcanism<sup>12</sup>. Finally, asthenospheric shear can directly induce upwelling, and thus volcanism, by interacting with lithospheric or asthenospheric viscosity heterogeneities. For example, asthenosphere flowing toward progressively thinner lithosphere experiences an upwelling component that can cause melting<sup>3,10,12</sup>. Alternatively, because asthenospheric shear tends to become concentrated within low-viscosity 'pockets' that are embedded within the asthenosphere, shearing of viscously heterogeneous asthenosphere can excite 'shear-driven upwelling' that can induce volcanism<sup>18</sup>. These mechanisms predict more intraplate volcanism above rapidly shearing regions of the asthenosphere. Here we test this prediction by comparing the geographic distribution of intraplate volcanism with model predictions of asthenospheric magnitudes.

We estimated the magnitude of shear in the present-day asthenosphere using a model of global mantle flow<sup>21</sup> driven by surface plate motions and mantle density heterogeneity (see Supplementary Information). Asthenospheric shear amplitudes exhibit large geographic variations because the magnitudes and directions of upper mantle flow and surface-plate motions vary spatially (Supplementary Fig. S1). Beneath continents, shear amplitudes range from nearly zero shear beneath most of Africa, Asia and eastern North America to 5–8 cm yr<sup>-1</sup> beneath western North and South America, and the fast-moving Australian continent (Fig. 1a, colours). Shear-amplitude variations are typically larger beneath the Pacific and Indian basins (Fig. 2a, colours), where surface-plate motions are faster than they are for continents.

To determine whether continental intraplate volcanism preferentially occurs in regions of high asthenospheric shear, we plotted 3,760 volcanic samples from the [www.earthchem.org](http://www.earthchem.org) database that met the criteria of being recent (<10 Myr old), intraplate (>300 km from a volcanic plate boundary) and classified as basalt (Supplementary Fig. S2; see Supplementary Information). We then corrected for sample duplication by designating continental areas within 100 km of a sampled location as regions of 'intraplate volcanism' (Fig. 1a; see Supplementary Information). The average shear magnitude for all such regions is 3.3 cm yr<sup>-1</sup>, which is 1.74 times higher than the intraplate continental average of 1.9 cm yr<sup>-1</sup>. In fact, the distribution of shear for all intraplate volcanism areas is bimodal and contains a large high-shear peak that notably skews the intraplate volcanism distribution toward high shear magnitudes (Fig. 1b). For example, 64% of the intraplate volcanism occurs in regions overlying asthenosphere shearing faster than 3.0 cm yr<sup>-1</sup>, which underlies only 18% of intraplate continental area. Similarly, 18.4% of the continental area that overlies asthenosphere shearing faster than 6.0 cm yr<sup>-1</sup> contains volcanism, which

<sup>1</sup>Department of Geology & Geophysics, School of Ocean and Earth Science and Technology, University of Hawaii at Manoa, Honolulu, Hawaii 96822, USA,

<sup>2</sup>Department of Geoscience, University of Nevada Las Vegas, Las Vegas, Nevada 89154, USA. †Present addresses: Center for Advanced Studies, Norwegian Academy of Letters and Sciences, NO-0271, Oslo, Norway (C.P.C.); Department of Geological Sciences, Brown University, Providence, Rhode Island 02912, USA (T.A.B.). \*e-mail: [clintc@hawaii.edu](mailto:clintc@hawaii.edu).

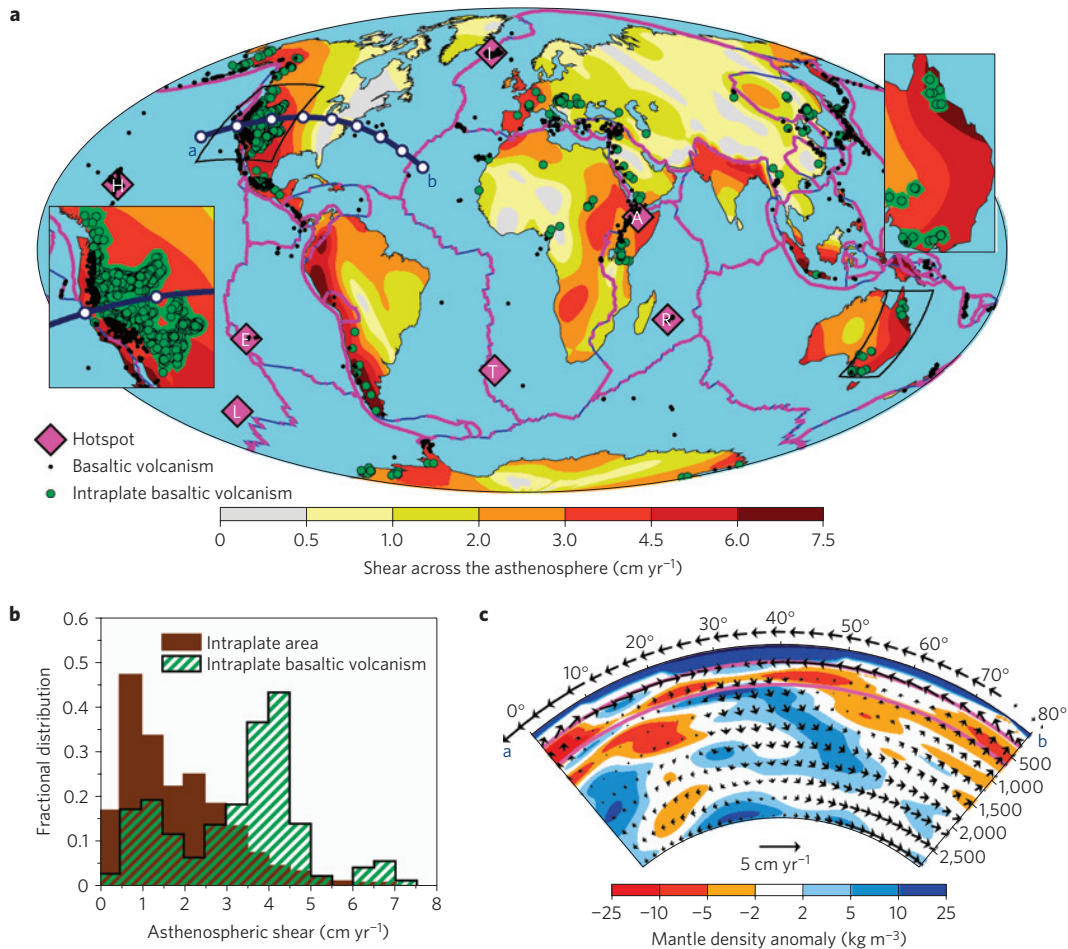


**Figure 1 | Spatial correlation between asthenospheric shear and continental intraplate volcanism.** **a**, Background colours show asthenospheric shear magnitude. Recent basaltic volcanism locations are denoted as continental intraplate (green circles) or other (black dots) (see Supplementary Information). Regions less than 100 km from intraplate volcanism are denoted (insets; green area), as are major hotspots<sup>1</sup> (pink diamonds: A = Afar, C = Caroline, E = Easter, H = Hawaii, I = Iceland, L = Louisville, R = Réunion, S = Samoa, T = Tristan) and volcanic plate boundaries (pink lines). **b**, Asthenospheric shear distribution for all intraplate areas (brown) compared with the distribution for regions containing intraplate volcanism (green hatched). **c**, Mantle density heterogeneity (colours), flow velocity (arrows in panel) and plate motions (arrows above panel) across western North America (section in **a**).

represents a volcanism density nearly five times that of intraplate continental areas overall.

To test the probability that the observed co-location of intraplate volcanism and shear might result from random chance, we computed the *p*-value (see Methods) by testing 10,000 random reorientations (Supplementary Fig. S3) of the global asthenospheric shear pattern and recomputing the shear distributions of Fig. 1b for each. We measured an average shear for intraplate volcanism at least as extreme as our observed measure (that is,  $\geq 1.74$  times the intraplate average) only 3.75% of the time. Additionally, the Kolmogorov–Smirnov statistical test (see Methods) shows that the chance that the observed volcanism shear distribution could result from fortuitous random sampling of the intraplate distribution is less than 5% if the former is formed from only six or more independent points (Supplementary Fig. S4). Given that there are significantly more than six independent regions of intraplate volcanism (Fig. 1a), these statistical tests indicate that the prevalence of intraplate volcanism in regions of high shear is not a chance occurrence.

The continental regions with the greatest asthenospheric shear are western North America and eastern Australia, both of which feature extensive intraplate basaltic volcanism<sup>2–4</sup>. High-amplitude shearing beneath Australia has been inferred from

seismic anisotropy and is explained by the rapid northward motion of that continent<sup>22</sup>. Western North America's high asthenospheric shear is also anisotropically inferred<sup>23</sup> and is induced by westward North American plate motion above eastward upper-mantle flow towards the Farallon slab downwelling (Fig. 1c). Basaltic volcanism in Antarctica, South America, and Europe also tends to occur in regions of high shear (Fig. 1a). There are a few important regions of intraplate volcanism in Africa and Asia that occur in regions with low shear, but these regions represent a minority.

Seamounts, found on the sea floor of every ocean basin, are the result of intraplate volcanism, but many were formed long ago when shear patterns were different. To designate submarine areas of recent intraplate volcanism (see Supplementary Information), we consider seamounts from a global survey<sup>24</sup> that reside on sea floor younger than 10 Myr (Fig. 2a). As we found above for continental regions, average shear beneath submarine volcanism is greater than it is beneath young sea floor generally (by a factor of 1.45), and its bimodal distribution is also skewed toward higher shear (Fig. 2b). For example, asthenosphere shearing faster than  $8.0 \text{ cm yr}^{-1}$  accounts for only 19% of young seafloor area but underlies 43% of sea floor near young seamounts. Computing the *p*-value for submarine volcanism (see Methods), we found that only 2.76% of asthenospheric shear reconfigurations

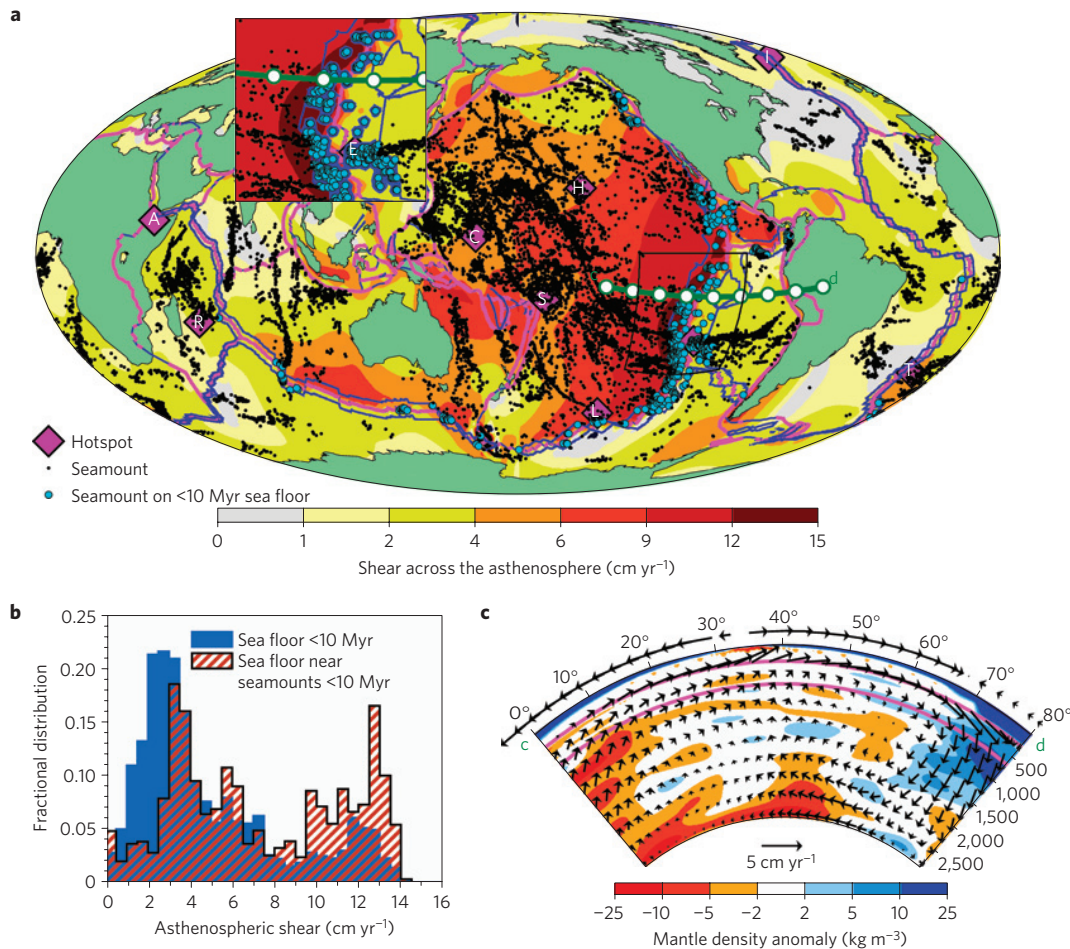


**Figure 2 | Spatial correlation between asthenospheric shear and seamount volcanism. a**, Locations of seamounts<sup>24</sup> residing on sea floor less than 10 Myr old (blue circles) and those on older sea floor (black dots). Asthenospheric shear amplitude (background colours, note the difference from Fig. 1a), intraplate volcanism regions (inset; blue area), hotspots (A = Afar, C = Caroline, E = Easter, H = Hawaii, I = Iceland, L = Louisville, R = Réunion, S = Samoa, T = Tristan) and plate boundary locations are as in Fig. 1a. **b**, Asthenospheric shear distribution for sea floor younger than 10 Myr (blue) compared with the distribution for regions within 100 km of a seamount (red hatched). **c**, Mantle flow patterns (depicted as in Fig. 1c, except that plate-motion-arrow lengths have been reduced by half) across the EPR (section in **a**).

yield average sub-seamount shear at least 1.45 times the young seafloor average, and only 0.034% satisfy both continental and submarine amplifications simultaneously (Supplementary Fig. S3). The Kolmogorov–Smirnov test indicates that the probability that the observed seamount shear distribution could arise by chance is less than 5% if this distribution is defined by 18 or more independent points (Supplementary Fig. S4). For comparison, there are more than 30 times this number of young seamounts, although perhaps not all are independent. These tests strongly indicate that seamount volcanism, similarly to continental volcanism, occurs preferentially above rapidly shearing asthenosphere. Note that our method defines the seamount track east of the Easter Island hotspot as a region of intraplate volcanism (Fig. 2a, inset). If these seamounts, which sit above weakly shearing Nazca asthenosphere, were excluded as products of the Easter Island plume<sup>3</sup>, then the bimodal shear distribution for intraplate volcanism would become even more skewed toward higher shear magnitudes (Fig. 2b).

The greatest density of seamounts on young sea floor occurs west of the East Pacific Rise (EPR), where the asthenosphere is shearing more rapidly than anywhere else on the planet (Fig. 2a). This rapid shear, which can reach up to  $14 \text{ cm yr}^{-1}$ , results from westward Pacific plate motion opposed by eastward upper-mantle flow from South Pacific upwelling toward South American subduction downwelling (Fig. 2c). By contrast, east of the EPR the Nazca

plate and underlying mantle both move eastward, which reduces asthenospheric shear considerably and correlates with notably fewer seamounts (Fig. 2a, inset). This asymmetry in seamount density across the EPR has been noted previously<sup>9</sup>, is similar to asymmetry across the Juan de Fuca ridge<sup>11</sup> and indicates excess melt on the western side of these ridges. This melting asymmetry may result from eastward-directed pressure-driven asthenospheric flow that induces upwelling beneath the (eastward-thinning) Pacific plate<sup>10</sup>. Sampling of less-depleted mantle on the Pacific flank by westward ridge migration may also yield asymmetric melting<sup>11</sup>, but melting calculations suggest that this effect is small<sup>10</sup>. Here we suggest an alternative explanation: that viscosity heterogeneity beneath both plates is ubiquitous, but is able to excite more vigorous shear-driven upwelling<sup>18</sup>, and associated melting, on the EPR's western flank because shearing amplitudes are significantly higher there.

Pacific seamounts away from ridges result from past intraplate volcanism, and are therefore useful for constraining the time dependence of this volcanism. Using a database of Pacific seamount ages<sup>25</sup> (Supplementary Fig. S5), we estimated (see Supplementary Information) the average seamount volume density on the Pacific plate, as a function of seafloor age, for seamounts that formed near the ridge axis (on sea floor 0–10 or 10–20 Myr old), and for those that formed on older sea floor (20–45 or >45 Myr old) (Fig. 3). The time dependence of near-ridge seamount volume density roughly

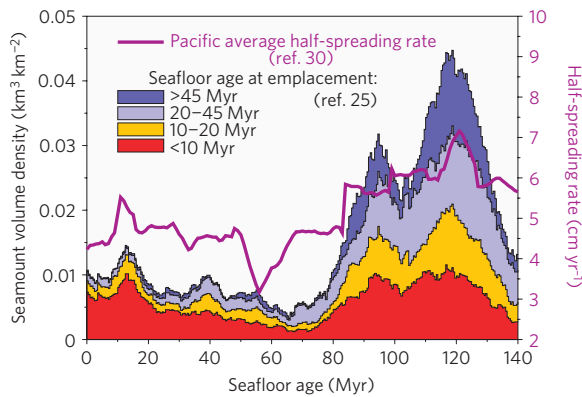


**Figure 3 | Temporal correlation between seamount density and spreading rate for the Pacific Basin.** The coloured regions (left axis) show seamount volume density (see Supplementary Information) on the Pacific plate as a function of present-day seafloor age, for four bins of seafloor age at the time of seamount emplacement<sup>25</sup>. Emplacement ages younger than underlying sea floor indicate uncertainty in age estimates for individual seamounts; this uncertainty is reduced here because groups of seamounts are considered in aggregate<sup>25</sup>. The purple curve (right axis) shows the average Pacific basin half-spreading rate as a function of seafloor age, computed by averaging seafloor spreading rates measured along Pacific basin isochrons that are less than 10 Myr old in a recent seafloor age reconstruction<sup>30</sup>.

correlates with variations in Pacific basin spreading rates (Fig. 3). In particular, both spreading rates and seamount emplacement rates were most elevated before 80 Myr, minimized around 60 Myr, and then increased to a local maximum at ~10 Myr. Average spreading rate should be correlated with Pacific plate velocity and therefore also with the amplitude of asthenospheric shear. Thus, the correlation of seamount production and seafloor spreading rates (Fig. 3) further supports the idea that intraplate volcanism is linked to rapid asthenospheric shear.

Intraplate volcanism does not occur above all rapidly shearing asthenosphere (for example, central eastern Australia), nor is high shear predicted beneath every intraplate volcano (for example, Cameroon line in eastern Africa). Thus, although high shear promotes intraplate volcanism, it must do so in conjunction with other factors (for example, viscosity heterogeneity and near-solidus asthenosphere), some of which occasionally generate volcanism in relatively low-shear environments. High shear may also occur on scales smaller than can be resolved by global flow models<sup>21</sup>. For example, slabs may significantly alter flow patterns regionally beneath mobile belts<sup>6</sup>, and lateral flow of upwelling mantle beneath the variable-thickness lithosphere of Africa may be associated with recent magmatism there<sup>7</sup>.

The presence of rapid shear beneath intraplate volcanism occurring in a variety of lithospheric and geologic settings suggests that the driving mechanism for this volcanism lies in the asthenosphere. Lithospheric mechanisms, such as cracking<sup>13,14</sup> or convective destabilization<sup>15–17</sup>, may be excited by asthenospheric shear through basal tractions or shear weakening, but the positioning of volcanism above shearing may be degraded by efficient lateral transmission of elastic stresses<sup>19</sup> and by the relative stability of younger, thinner lithosphere<sup>16,17,20</sup> (for example, beneath the EPR or western North America). By contrast, asthenospheric shear-driven upwelling predicts correlated volcanism and shear if viscosity heterogeneity is present<sup>18</sup>. Compositional heterogeneity may be ubiquitous beneath ridges regardless of relatively uniform ridge basalt composition<sup>26</sup>, and beneath some continents (including eastern Australia<sup>3,27</sup> and western North America<sup>28</sup>). Such pervasive heterogeneity, especially when associated with mineral hydration<sup>28</sup>,

may induce viscosity variations<sup>29</sup> that excite upwelling only in regions of high shear. If shear-driven upwelling explains the correlation between high shear and intraplate volcanism, then patterns of global mantle convection control most low-volume basaltic intraplate volcanism on Earth.

## Methods

To quantify the statistical significance of a measured difference between two distributions, we computed the *p*-value, which expresses the probability that the measured difference between the distributions, or a larger one, could arise if the two distributions were unrelated. To measure the *p*-value, we randomly re-oriented the observed pattern of asthenospheric shear (Supplementary Fig. S1) on the Earth's surface 10,000 times, so that each asthenospheric shear orientation is necessarily unrelated to the locations of intraplate volcanism on the Earth's surface, which we leave in place. The new orientations were chosen by carrying out uniformly distributed random rotations of the asthenospheric shear pattern (Supplementary Fig. S3). For each orientation, we compared the distribution of shear for intraplate (or young sea floor) areas to the new shear distribution for intraplate volcanic (or seamount-proximal) regions (that is, we recomputed the distributions of Figs 1b and 2b using the new orientation of asthenospheric shear on the Earth's surface). The *p*-value is the fraction of tests that produce shear distributions for intraplate volcanism and for the background intraplate area that differ by at least as much as is observed for the present-day Earth (Figs 1b and 2b). We used the ratio of the mean value of each distribution to express this difference (1.74 for continental intraplate volcanism and 1.45 for young seamounts), although other measures (for example, the difference in the average value between the distributions, or the fraction of the shear distribution for volcanism that lies above the average value of the shear distribution for the background area) produce similar results. Note that the *p*-value test does not depend on the number of independent volcanism regions that compose the shear distributions (Figs 1b and 2b), and it is still valid even if sampling of intraplate volcanism regions is not complete or evenly distributed.

The Kolmogorov–Smirnov test also quantifies the probability that an observed difference between two distributions might arise by chance, but it requires prior knowledge of *N*, which is the number of independently sampled points that form the observed distribution. Although our intraplate volcanism databases contain large numbers of volcanic locations (3,760 locations for basaltic volcanism and 558 for young seamounts), not all of these locations are independent and it is difficult to estimate *N* for our distributions. An upper bound of *N* ~ 100 can be obtained by dividing the length of Earth's two-sided ridge system (~100,000 km; we use both sides because they are independent) by the possible length scale of mantle flow variations (~1,000 km here because we estimate asthenospheric shear from a flow model<sup>21</sup> driven by tomographically inferred mantle density heterogeneity up to spherical harmonic degree 20). Maximum *N* should be much larger for continental volcanism because continents cover a larger area than young (<10 Myr) sea floor. Because we do not know *N*, we carry out the Kolmogorov–Smirnov test for a range of values of *N* by first dividing the shear distribution for regions of intraplate volcanism into *N* bins of equal area. The boundaries of these bins are determined by dividing the *y* axis of the cumulative distribution function into *N* equal parts, and then projecting these parts into *N* bins in shear amplitude. We then randomly select values of shear within each bin (so that the distribution arising from these *N* samples mimics the observed distribution of shear above intraplate volcanism). Carrying out the Kolmogorov–Smirnov test on these values, and repeating the process 10,000 times to measure average statistics (using double or quadruple this number does not change our results), we determine the chances that a given (continental or oceanic) distribution of intraplate volcanism might be obtained by random sampling, as a function of *N* (Supplementary Fig. S4). In doing so, we determine the minimum number of samples that are needed so that there is less than a 5% chance that the shear distribution for intraplate volcanism locations is drawn from the shear distribution for all intraplate regions.

Received 6 September 2010; accepted 14 February 2011; published online 20 March 2011

## References

1. Courtillot, V., Davaille, A., Besse, J. & Stock, J. Three distinct types of hotspots in the Earth's mantle. *Earth Planet. Sci. Lett.* **205**, 295–308 (2003).
2. Valentine, G. A. & Hirano, N. Mechanisms of low-flux intraplate volcanic fields—Basin and Range (North America) and northwest Pacific Ocean. *Geology* **38**, 55–58 (2010).
3. Demidjuk, Z. *et al.* U-series isotope and geodynamic constraints on mantle melting processes beneath the Newer Volcanic Province in South Australia. *Earth Planet. Sci. Lett.* **261**, 517–533 (2007).
4. Johnson, R. W. *Intraplate Volcanism in Eastern Australia and New Zealand* (Cambridge Univ. Press, 1989).
5. Gans, P. B. & Bohrsen, W. A. Suppression of volcanism during rapid extension in the Basin and Range Province, United States. *Science* **279**, 66–68 (2007).

6. Faccenna, C. & Becker, T. W. Shaping mobile belts by small-scale convection. *Nature* **465**, 602–605 (2010).
7. Ebinger, C. J. & Sleep, N. H. Cenozoic magmatism throughout east Africa resulting from impact of a single plume. *Nature* **395**, 788–791 (1998).
8. Forsyth, D. W., Harmon, N., Scheirer, D. S. & Duncan, R. A. Distribution of recent volcanism and the morphology of seamounts and ridges in the GLIMPSE study area: Implications for the lithospheric cracking hypothesis for the origin of intraplate, non-hot spot volcanic chains. *J. Geophys. Res.* **111**, B11407 (2006).
9. Scheirer, D. S., Forsyth, D. W., Cormier, H.-M. & Macdonald, K. C. Shipboard geophysical indications of asymmetry and melt production beneath the East Pacific Rise near the MELT Experiment. *Science* **280**, 1221–1224 (1998).
10. Conder, J. A., Forsyth, D. W. & Parmentier, E. M. Asthenospheric flow and asymmetry of the East Pacific Rise, MELT area. *J. Geophys. Res.* **107**, 2344 (2002).
11. Davis, E. E. & Karsten, J. L. On the cause of the asymmetric distribution of seamounts about the Juan de Fuca ridge: Ridge-crest migration over a heterogeneous asthenosphere. *Earth Planet. Sci. Lett.* **79**, 385–396 (1986).
12. Raddick, M. J., Parmentier, E. M. & Scheirer, D. S. Buoyant decompression melting: A possible mechanism for intraplate volcanism. *J. Geophys. Res.* **107**, 2228 (2002).
13. Turcotte, D. L. & Oxburgh, E. R. Intra-plate volcanism. *Phil. Trans. R. Soc. Lond. A* **288**, 561–579 (1978).
14. McKenzie, D. & Bickle, M. J. The volume and composition of melt generated by extension of the lithosphere. *J. Petrol.* **29**, 625–679 (1988).
15. King, S. D. & Ritsema, J. African hot spot volcanism: Small-scale convection in the upper mantle beneath cratons. *Science* **290**, 1137–1140 (2000).
16. Elkins-Tanton, L. T. Continental magmatism, volatile recycling, and a heterogeneous mantle caused by lithospheric gravitational instabilities. *J. Geophys. Res.* **112**, B03405 (2006).
17. Ballmer, M. D., van Hunen, J., Ito, G., Bianco, T. A. & Tackley, P. J. Intraplate volcanism with complex age–distance patterns: A case for small-scale sublithospheric convection. *Geochem. Geophys. Geosyst.* **10**, Q06015 (2009).
18. Conrad, C. P., Wu, B., Smith, E. I., Bianco, T. A. & Tibbetts, A. Shear-driven upwelling induced by lateral viscosity variations and asthenospheric shear: A mechanism for intraplate volcanism. *Phys. Earth Planet. Int.* **178**, 162–175 (2010).
19. Naliboff, J. B., Conrad, C. P. & Lithgow-Bertelloni, C. Modification of the lithospheric stress field by lateral variations in plate–mantle coupling. *Geophys. Res. Lett.* **36**, L22307 (2009).
20. Molnar, P., Houseman, G. A. & Conrad, C. P. Rayleigh–Taylor instability and convective thinning of mechanically thickened lithosphere: Effects of non-linear viscosity decreasing exponentially with depth and of horizontal shortening of the layer. *Geophys. J. Int.* **133**, 568–584 (1998).
21. Conrad, C. P. & Behn, M. D. Constraints on lithosphere net rotation and asthenospheric viscosity from global mantle flow models and seismic anisotropy. *Geochem. Geophys. Geosyst.* **11**, Q05W05 (2010).
22. Debayle, E., Kennett, B. & Priestley, K. Global azimuthal seismic anisotropy and the unique plate-motion deformation of Australia. *Nature* **433**, 509–512 (2005).
23. Becker, T. W., Schulte-Pelkum, V., Blackman, D. K., Kellogg, J. B. & O’Connell, R. J. Mantle flow under the western United States from shear wave splitting. *Earth Planet. Sci. Lett.* **247**, 235–251 (2006).
24. Wessel, P. Global distribution of seamounts inferred from gridded Geosat/ERS-1 altimetry. *J. Geophys. Res.* **106**, 19431–19441 (2001).
25. Hillier, J. K. Pacific seamount volcanism in space and time. *Geophys. J. Int.* **168**, 877–889 (2007).
26. Ito, G. & Mahoney, J. J. Flow and melting of a heterogeneous mantle: 2. Implications for a chemically non-layered mantle. *Earth Planet. Sci. Lett.* **230**, 47–63 (2005).
27. Fishwick, S., Heintz, M., Kennett, B. L. N., Reading, A.M. & Yoshizawa, K. Steps in lithospheric thickness within eastern Australia, evidence from surface wave tomography. *Tectonics* **27**, TC4009 (2008).
28. Dixon, J. E., Dixon, T. H., Bell, D. R. & Malservisi, R. Lateral variation in upper mantle viscosity: Role of water. *Earth Planet. Sci. Lett.* **222**, 451–567 (2004).
29. Hirth, G. & Kohlstedt, D. L. in *Inside the Subduction Factory* (ed. Eiler, J.) 83–105 (Geophys. Monogr., Vol. 138, American Geophysical Union, 2003).
30. Müller, R. D., Sdrolias, M., Gaina, C., Steinberger, B. & Heine, C. Long-term sea-level fluctuations driven by ocean basin dynamics. *Science* **319**, 1357–1362 (2008).

### Acknowledgements

We thank S. King and J. Hillier for comments that improved the manuscript. This work was supported by NSF grant OCE-0937319, the Nevada Agency for Nuclear Projects and the Clark County Department of Comprehensive Planning, Nuclear Waste Division. This is SOEST contribution 8081.

### Author contributions

C.P.C., T.A.B. and E.I.S. developed the statistical comparisons between continental volcanism and asthenospheric shear; C.P.C. and P.W. developed the statistical comparisons between seamount databases, asthenospheric shear and seafloor spreading rates; C.P.C. prepared the manuscript with input, comments and review from all authors.

### Additional information

The authors declare no competing financial interests. Supplementary information accompanies this paper on [www.nature.com/naturegeoscience](http://www.nature.com/naturegeoscience). Reprints and permissions information is available online at <http://npg.nature.com/reprintsandpermissions>. Correspondence and requests for materials should be addressed to C.P.C.